

Notes on the VPPEM electron optics

Raymond Browning

2/9/2015

We are interested in creating some rules of thumb for designing the VPPEM instrument in terms of the interaction between the field of view at the sample, and the energy resolution obtainable from a concentric hemispherical analyzer (CHA). When we are considering the image of the sample entering the CHA through the entrance slits, we have to understand that the image at the magnetic field exit aperture is not a simple angular image, it also has a spatial dimension. This spatial dimension is significant because there is a magnification of the field of view at the sample by the decrease in the magnetic field as the electrons move away from the strong central field. The angular image is also rotated with respect to the spatial image. Therefore, when we calculate the energy resolution when this image is projected by the input lens into the entrance slit of the CHA, we have to consider the combination of these image properties.

We will initially treat the angular image and the spatial image independently. The angular image size is determined by the angle made by the off-axis momentum gained from the vector potential field as the electron exits the magnetic field, and the forward momentum of the exiting electron.

$$\theta = \frac{p_a}{p_f} \quad (1)$$

Where the off-axis momentum is, from conservation of momentum:

$$p_a = -eA \quad (2)$$

And the forward momentum is:

$$p_f = \sqrt{2meE} \quad (3)$$

Where E is the energy of the electron in eV.

The vector potential A at radius r in a magnetic field B in Tesla will be:

$$A = \frac{rB}{2} \quad (4)$$

Combining these four equations gives:

$$\theta = k \frac{rB}{\sqrt{E}} \text{ radians} \quad (5)$$

Where $k = 1.48 \times 10^5 = (0.125 m/e)^{0.5}$.

The spatial magnification M of the magnetic field acting as a projection lens (a Turner lens) depends on the square root of the ratio of the initial magnetic field at the sample field at the sample B_s , and the final exit magnetic field B_e :

$$M = \sqrt{\frac{B_s}{B_e}} \quad (6)$$

If we have the maximum field of view at the sample as r_s , then we have the maximum angle in radians:

$$\theta_{max} = k \frac{r_s B_e}{\sqrt{E}} \sqrt{\frac{B_s}{B_e}} = k \frac{r_s \sqrt{B_e B_s}}{\sqrt{E}} \quad (7)$$

For example with a 20 T initial field, a 100 Gauss exit field, an exit electron energy of 100 eV, and a 5 micron half-field of view, then:

$$\theta_{max} = 3.3 \times 10^{-2} \text{ radians} \quad (8)$$

The energy resolution of a CHA is:

$$\frac{\Delta E}{E} = \frac{w}{2R} + \alpha^2 \quad (9)$$

Where w is the slit size, R is the center radius of the CHA, and α is the half angle of the electron entering the CHA.

Using the figure from equation 8, and a CHA input lens of 1:1 magnification with the same input and output energy, would give an energy resolution of approximately 910:1 from the angle, and nominally a projected image size of

450 microns. Taken together this would give an energy resolution of:

$$\frac{\Delta E}{E} = \frac{0.45}{2*200} + \frac{1}{910} = 1/450 \quad (10)$$

For a CHA with 200 mm radius. This is an energy resolution of 0.2 eV for 100 eV pass energy. Which is where we want to be for the VPPEM low energy imaging. Note we have chosen the figures to give approximately the same contribution from angle and image size.

The two main parameters we have control over are the electron exit energy, and the final magnetic field. We can also change the magnification of the input lens, but note that if we make this lens a demagnifying lens then the angle increases. Assuming the field of view ($2r$) just fits into the CHA entrance slit w , and combining equations 6, 7, and 9:

$$\frac{\Delta E}{E} = \frac{2r_s}{2R} \sqrt{\frac{B_s}{B_e}} + kr_s \frac{\sqrt{B_e B_s}}{\sqrt{E}} \quad (11)$$

Multiplying both sides by E , and collecting terms:

$$\Delta E = \frac{r_s}{R} \left(E \sqrt{\frac{B_s}{B_e}} + kR\sqrt{E} \sqrt{B_e B_s} \right) \quad (12)$$

From equation 12 it can be seen that for a fixed energy window the field of view is dependent on the size of the CHA. If the relative contributions of the magnification and angle are kept the same by changing the exit field strength then the field size scales as \sqrt{R} . Therefore, a larger CHA leads to a larger field of view. Reducing the exit energy will also increase the field of view. This will be true until the CHA overfills, as this will happen at about 0.1 radians the final energy we would use is in the region of 50 eV given our model up till now. But at this point we would need to consider the filling of the input lens, as spherical aberration will start to distort the image. There is also the issue of field curvature in the output

lens which will defocus the electron image at high angles.

The dependence on the exit field B_e is more complex. It would seem from our previous argument that it is useful to think of it acting in combination with the electron energy to manage the relative proportions of the spatial, and angular terms in equation 12.

Treating the angular and the spatial images independently gives us a guide to how to design the VPPEM. But to go further we need to combine the parameters of the magnetic field, input lens, CHA, and output lens.

As we have said, the output from the magnetic field is a combination of an angular, a spatial image, and a rotation. The formation of the angular image is driven by conservation of momentum from the vector potential field at the field termination. The spatial image has a magnitude determined by the magnification of the field of view by the change in magnetic field from the sample to the field termination. The rotation is part of the process of the formation of the angular image. The termination of the vector potential field produces both a transverse deflection across the optic axis, and a deflection away from the axis as the vector potential decreases along the axis of the magnet as it terminates. In fact, the spatial magnification which also produces a deflection away from the optical axis in the meridional plane is part of this process.

The actual mix of these effects is dependent on the shape of the magnetic field termination, how sharp the termination is, and the energy of the electrons. At lower energies, electrons stay longer in the field so that the spatial magnification is relatively larger. The angle of exit due to the off-axis deflection is also larger. At the same time the vector potential angular contribution at right angle to this deflection is smaller. The angular image rotation is therefore

less. The rotation is found from simulation to be between 30-60°, depending on the conditions.

As we have shown that tending towards lower energies is useful to increase the field of view, we should consider moving the operation of the microscope towards lower energies, and a greater contribution to the angular image from deflection in the meridional plane. The issue with this can be seen in figure 1 where the meridional (x) projection shows the trajectories moving away from the optic axis (z), where the transverse projection (y) shows the electron move across the axis. It can be seen that the apparent object positions for a subsequent lens are different for the different projections. The object source in the meridional plane is nearer the field, while transverse source position is farther out.

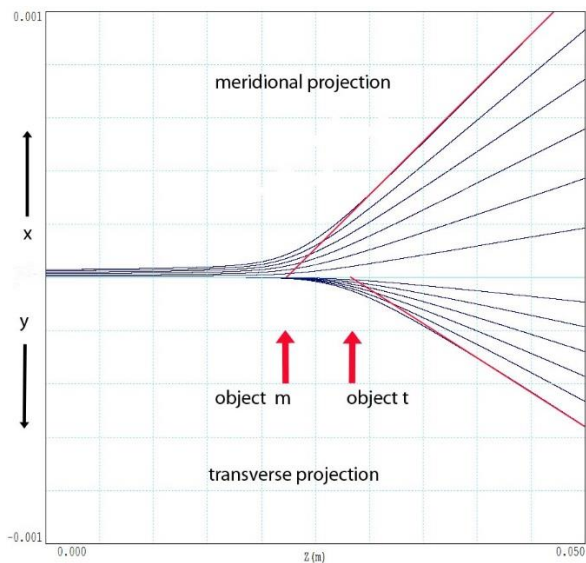


Figure 1. The apparent object positions in the meridional, and the transverse projections.

Naturally this double source makes it impossible to have a true focusing lens into the CHA. Therefore, we have described this as a condensing lens. The two sources mean that the condenser lens does not produce a crossover of the axis. This can be seen in the radial plot of an input lens shown in Figure 2.

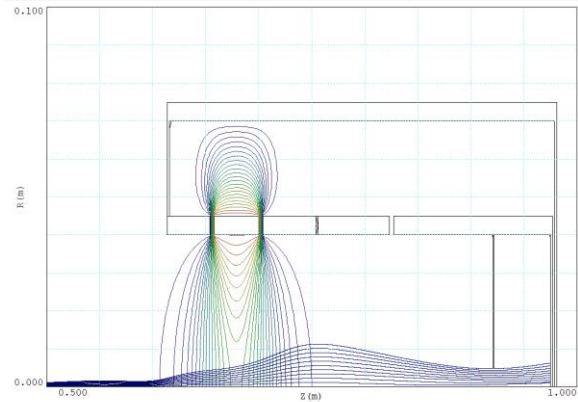


Figure 2. CHA input lens with spatial magnification, and lower entrance angle. This radial position shows that the trajectories do not cross over the axis.

It would appear that as we are using low energy electrons, and we have a large meridional plane contribution to the angular image anyway, it would be better to maximize one contribution over the other. This might make managing the condenser lens easier. There is also another design implication. To make the meridional plane angular contribution dominant the field termination can be made 'soft'. This means that the final aperture can be made larger, and thus magnetic imperfections in the soft iron ring used as the terminating aperture will not be so critical. We have found from the prototype that this is an important consideration.

To move forward with parameterizing the electron optics, and assuming that lower energy electrons will be used with a soft termination. I am going to assume that the relative contributions give a rotation away from the meridional plane of a maximum of 30° so that we can consider most of the angular effect are along this plane.

As the angle, and the spatial magnification are not independent equation 12 is only a guide to the CHA performance. To understand what the imaging properties of the CHA are we need to use the orbital equations.

If x_i and x_o are the distances of the incoming, and outgoing electron from the central radius R of the CHA we have:

$$\frac{x_o}{R} = -\frac{x_i}{R} + \frac{2\Delta E}{E} - \alpha^2 \quad (13)$$

Note that the angular term is always negative so that we have an unsymmetrical response to the image out of the field. When x_i is negative it can cancel the angular term, when it is positive it adds to the angular term. As x_i and the angle are correlated this means that the image has a nonlinear dispersion across the field of view.

Over the negative half of the field of view it is possible to cancel the dependence of the CHA response to distance, and angle using an appropriate choice of output parameters from the field, and the magnification of the CHA input lens. The energy resolution in the lower half of the image then only depends on the size of the output aperture w . The input slit only acts as a field, and angle stop. This has implications for the system design because we can now pass the photon beam through the alignment port of the CHA, and not be concerned with it having to pass through a narrow slit.

The field of view of the lower half of the field is now dependent on the largest angle that can be passed through the CHA. The largest deviation of the orbits due to the angle, assuming a low energy dispersion is approximately:

$$x_{max} = \alpha R \quad (14)$$

Thus for a 200 mm CHA with an inner hemisphere of 175 mm we have a maximum angle of 0.125 radians. This implies from equation 13 that the equivalent distance from the central orbit at the entrance x_i is -3 mm to cancel the energy shift. If we keep an input aperture that is symmetric around the central radius, we have an entrance slit of 6 mm in the dispersive plane, and we can then consider a 10 mm width in the non-dispersive plane. This size

slit should be sufficient room to pass through two photon beams canted at 5° .

We then have an unusual output image. The image is an angular image with a 3:5 ratio, a maximum angle 0.125 radians, and an energy window determined by the CHA output slit size in the dispersive plane. But the angular image is only in one direction from zero. We can now consider how this will be projected onto a real image plane by the CHA output lens.

We have previously modelled the output lens, but not with this unusual image.

Figure 3 shows our calculation for the current prototype instrument. The output image size is suggested from the microscope requirements. The requirements call for 1000 lines in the image. The minimum pixel size is set by the resolution of the micro channel plate. The resolution is typically in the 20-40 micron size for a chevron stack. This implies the output image will be 30-40mm in diameter.

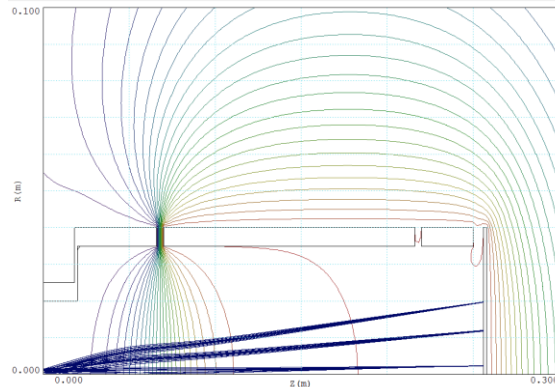


Figure 3. CHA Output lens for current prototype.

The solution shown in figure 3 uses a total length of 250mm fitting inside a 6" conflat, but it may be advantageous to extend the length, and width. The slit width is 2 mm, and this solution is only for the electrons in the dispersion plane.

The largest imaging aberration is due to field curvature at the image plane. There is some compensation for field curvature which is

achieved by slight overfilling of the lens. The compensation is only approximate. The solution shown in has approximately 1000 lines/image at the center of the field of view and 400 lines/image at the edge, of a 40 mm image.

The input for this solution was a uniform distribution of angles across the 2mm CHA exit slit. We need to use the actual angular and spatial distribution coming out of the CHA. This means we must calculate the full optical path from the magnet, through the CHA input lens, the CHA using the orbit equation of equation 13, the output slit dimensions, and the CHA output lens. As this is a significant amount of calculation we must leave this to a later time.

In conclusion we have some design outputs:

1. The magnetic field can have a 'soft' termination, and a thus a large aperture.
2. The CHA input aperture can be large, so that a canted dual photon beam can pass through it.
3. The microscope field of view is larger with a larger CHA.
4. The CHA energy resolution does not depend on angle or entrance slit size, only the exit slit size w in the dispersive plane need be considered. The CHA resolution is then:

$$\frac{\Delta E}{E} = \frac{w}{2R}$$

As we have completely changed the normal CHA design criteria set out in our earlier equations we need to confirm the validity of these observations with simulation of the complete optical system.